PRELIMINARY DESIGN OF AIRCRAFT WINGS FOR THE DYNAMIC LOADS IN LANDING

By

E. Rácz

Department of Aeronautics. Technical University. Budapest

1. Origins of the dynamic load

Requirements for aircraft design specify flying conditions for designing each part of the aircraft (wing, fuselage etc.). Earlier, and even now, the so specified service loads were applied to an aircraft assumed rigid; and, if the active forces were not in equilibrium, the balance was restored by inertia forces. This means that the load was considered to be static (or better pseudo-static, in view of the inertia forces).

An aircraft, however, is an elastic structure. If rapidly applied external forces are acting on such a structure, the mass particles of the structure will get into vibration, in addition to the translation and rotation, i.e. rigid body motions of the structure. The inertia forces from this vibration will result in dynamic load, the magnitude of which will depend upon the relation of the vibration characteristics of the structure (eigenfrequencies, mode shapes) and the time history of the external forces.

With aircraft wings, particularly in earlier times, it was unnecessary to take into consideration the dynamic load, owing to its small value. When, however, the safety factor was reduced gradually from the original value of 2 to 1.8 and then to 1.5 (accompanied by a relative decrease of the aircraft rigidity), and, at the same time, more and more slender wings were applied, for instance, on transport aircrafts, to increase the range, the importance of dynamic load has grown markedly.

The impact on the ground in landing and the gust in flight produce an extremely rapidly (within a few tenths of the second) increasing impulse load of considerable dynamic effect, whereas manoeuvre flight, for instance, can be taken as a slow process, producing only "static" load.

The slender wing of the big transport aircrafts, with rear-mounted engines (at the end of the fuselage) receiving its ultimate load mainly from the gust should be examined by all means for dynamic load from the gust; while the multi-engined, slender-winged bomber or transport aircrafts, as well as the fighter type aircrafts with wingtip tank, or tandem landing gear (attached to the fuselage) will meet danger first of all in the dynamic load from landing. With sailplanes both types of load are considerable because of their much

greater wing aspect ratio — compared to other aircrafts — and their landing wheel attached to the fuselage.

The following investigation of dynamic wing loads will be restricted to straight (other than swept back) wings; and only the flexural vibration of the wing will be considered, taken as a linear vibration. The wing being flexible, it forms a dynamic system of infinite number of degrees of freedom; its general flexural vibration can be produced from the superposition of the individual eigenvibrations. In each eigenvibration the wing can be considered as a system with one degree of freedom; therefore, as an introduction, the dynamic load on a system with one degree of freedom will be shortly summarized.
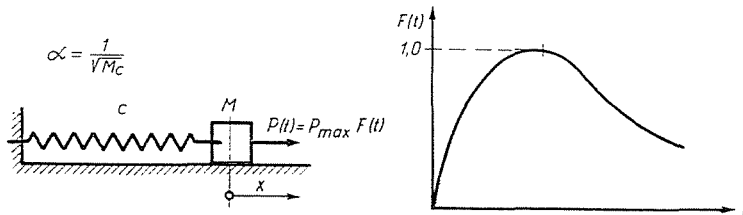

Fig. 1. Dynamic load on a one degree of freedom system

The displacement of mass M of a system with one degree of freedom, (Fig. 1) due to force $P(t) = P_{max} F(t)$ at time t with initial conditions: $x(0) = 0$ and $\dot{x}(0) = 0$, will be given by the known formula [1]:

$$x = \frac{P_{max}}{M\alpha} \int_0^t F(\tau) \sin \alpha (t - \tau)\, d\tau.$$

For a "static" load $P_{max} F(t)$, the displacement (for the same t value) would be:

$$x_{st} = c P_{max} F(t).$$

The inertia force producing the dynamic load can be expressed as:

$$D(t) = \frac{x - x_{st}}{c} = P_{max} \xi(t),$$

where

$$\xi(t) = \alpha \int_0^t F(\tau) \sin \alpha(t - \tau)\, d\tau - F(t). \tag{1}$$

Spring design requires the highest value of the overall load: $T(t) = P(t) + D(t)$.

As to the aircraft wing, its general flexural vibration is given, as mentioned, by the superposition of the eigenvibrations. Since the wing load is symmetrical as a rule, only the symmetrical eigenvibrations must be taken into consideration.

The amplitude change of the ith eigenvibration along the wing span can be written as:

$$y_i(z) = \eta_i(z) \cdot H_i ,$$

where $\eta_i(z)$ is the *mode shape normalized for unit amplitude of the wing section in the symmetry plane, the so-called root section,* while H_i is the factor expressing the real displacement of the root section.
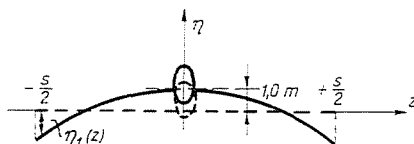

Fig. 2. Normalized mode shape of the first eigenvibration

Owing to the equilibrium of the inertia forces during the vibration of the wing, the aircraft represents a free system, i.e. its centre of gravity remains fixed in space, so that:

$$\int_{-s/2}^{+s/2} m(z)\, y_i(z)\, dz = 0 = \int_{0}^{s/2} m(z)\, \eta_i(z)\, dz \quad (i = 1, 2, 3 \ldots) , \tag{2}$$

where $m(z)$ is the specific mass (referred to unit length) along the wing span

Fig. 2 shows the normalized mode shape of the first eigenvibration.

The transient stresses of the wing caused by the impact force are examined by the method of WILLIAMS [2]. According to this method the stresses on the rigid wing are calculated segregately and to these, the dynamic stresses arising from the vibrations will be added. The quickly convergent method of WILLIAMS gives a better result than most of the other methods do, if, as in the present case, the investigation can be restricted to some of the lowest eigenvibrations [3, 4].

The time dependent distributed load on the rigid wing can be written in the form:

$$p(z, t) = p(z)\ F(t),$$

since generally (and always in landing) it varies with time in the same way along the span of the wing, i.e. it is independent of the motion of the wing sections.

$p(z)$ is the maximum distributed load from the pseudo-static force system, which can be written as

$$p(z) = \frac{dP_{\max}}{dz} - \frac{P_{\max}}{M} m(z) \, .$$

Here $P_{\max}$ is the maximum of the resultant impact force (thus $dP_{\max}/dz$ is the distributed impact force); M is the mass of the aircraft (hence the second term is the distributed mass force). Earlier, the wing was designed for stresses from this system of forces and from the initial system of forces in equilibrium (where the weight of the aircraft is equal to the lift) usually in stationary flight (level flight or gliding flight) preceding the attack of the impact force. (Further on we shall not deal with this latter system of forces.)

For investigating the dynamic load on the flexible wing the load $p(z)$ should be resolved into the sum of loads distributed similarly to the inertia force load in the eigenvibrations of the wing, since eigenvibrations can only be excited by loads similar in distribution to the inertia force distribution of the examined eigenvibration. Thus

$$p(z) = \sum_{i=1}^{\infty} q_i(z) \, ,$$

where

$$q_i(z) = m(z) \, \alpha_i^2 \, y_i(z) = m(z) \, \alpha_i^2 \, \eta_i(z) \, H_i \, .$$

α_i is the circular frequency of the ith eigenvibration. Comparing the two above expressions of $p(z)$:

$$\frac{dP_{\max}}{dz} - \frac{P_{\max}}{M} m(z) = m(z) \sum_{i=1}^{\infty} \alpha_i^2 \, \eta_i(z) \, H_i \, . \tag{3}$$

For determining H_i let Eq. (3) be multiplied by $\eta_i(z)$, and integrated along the wing span. Then, with regard to the principle of motion of mass-center and the orthogonality of eigenvibrations, the following relation holds:

$$\int_{-s/2}^{+s/2} \frac{dP_{\max}}{dz} \, \eta_i(z) \, dz = \alpha_i^2 \, H_i \int_{-s/2}^{+s/2} m(z) \eta_i^2(z) dz,$$

hence:

$$H_i = \frac{\displaystyle\int_{-s/2}^{+s/2} \frac{dP_{\max}}{dz} \, \eta_i(z) \, dz}{\alpha_i^2 \displaystyle\int_{-s/2}^{+s/2} m(z) \, \eta_i^2(z) \, dz} \, . \tag{4}$$

The ith eigenvibration is excited by the component $q_i(z)$ only; the distributed dynamic load, by analogy to the system with one degree of freedom, will be:

$$\frac{dD}{dz} F(t) = q_i(z)\, \xi_i(t)\,,$$

where

$$\xi_i(t) = \alpha_i \int_0^t F(\tau) \sin \alpha_i(t - \tau)\, d\tau - F(t)\,. \tag{5}$$

The resultant time dependent distributed load on the flexible wing will be:

$$p_R(z, t) = p(z)\, F(t) + \sum_{i=1}^{\infty} q_i(z)\, \xi_i(t) =$$

$$= \left[\frac{dP_{\max}}{dz} - \frac{P_{\max}}{M}\, m(z) \right] F(t) + m(z) \sum_{i=1}^{\infty} \alpha_i^2\, \eta_i(z)\, H_i\, \xi_i(t) \tag{6}$$

(superposed the initial equilibrium system of forces).

For a load analysis — according to (6) — the vibration data (eigenfrequencies, mode shapes), i.e. the actual construction of the wing must be known. This means that the calculation can be made only for the completely designed wing. This really used to be the case, the wing designed and constructed for static loads was subsequently examined for dynamic loads and, carrying out the emerging structural modifications, the calculation was repeated, sometimes in several stages.

2. Vibration characteristics of the "standard" wing

The resulting considerable computation work can much be reduced, keeping in mind that mass and second moment of area distribution of the aircraft wings (without major concentrated masses, e.g. engines) show a certain regularity. It can be assumed at a fair approximation that the specific mass is proportional to the square of the cord ratio, while the second moment of area to its fourth power (taking $c_y = $ const., these suppositions are rather obvious). For the most frequent trapezoid wing with taper ratio $h_v/h_0 = \zeta$ it can be written (Fig. 3a):

$$\left. \begin{aligned} h &= h_0 \left[1 - (1 - \zeta)\, \bar{z} \right] \\[2mm] m &= m_0 \left(\frac{h}{h_0} \right)^2 = m_0 \left[1 - (1 - \zeta)\, \bar{z} \right]^2 \\[2mm] J &= J_0 \left(\frac{h}{h_0} \right)^4 = J_0 \left[1 - (1 - \zeta)\, \bar{z} \right]^4 \end{aligned} \right\} \tag{7}$$

where h_0, m_0 and J_0 are the data of the root section, and $\bar{z} = 2z/s$.

In practice, the following procedure can be applied. Once and for all we determine the first two or three lowest eigenfrequencies and the pertaining normalized mode shapes of the standard wing (Fig. 3b), in a symmetrical free vibration for some practical values of taper ratio ζ and mass ratio φ (see Fig. 4b). Then in a given case the root section of the wing is designed for both the shear force and flexural moment due to static load. The sheet thickness is governed by the value of the similarly known torque acting in the root section.
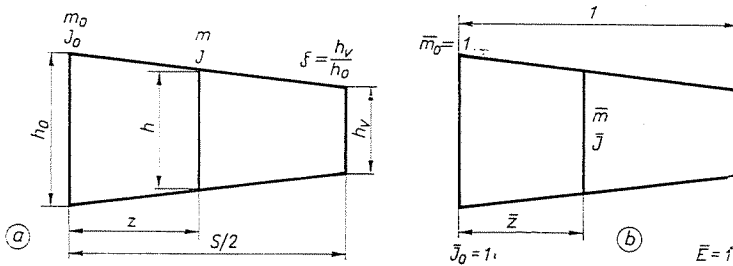

Fig. 3. Characteristics of the wing and "standard wing"

Thus the m_0 and J_0 values* of the wing are obtained. Now, if the wing is considered to have standard wing characteristics, its eigenfrequencies and mode shapes can be determined from the known data of the standard wing by interpolation and simple calculation. Hereafter, the dynamic load can be estimated, from which the maximum values of both the "dynamic" root bending moment and the shear force varying with time can be obtained. The root section will then be redesigned for the maximum stress obtained as above, leading to the values m_1 and J_1. The procedure converges rapidly and after one or two steps the final maximum distributed load of the wing sections is arrived at, for which the detailed structural design of the wing will be made. Finally, the ready designed wing will be put under full dynamic analysis, now with due consideration of the actual mass and second moment of area distribution. The preliminary approximation excludes the necessity of further structural modifications (or, only to a very small extent, if any).

The first two eigenfrequencies and normalized mode shapes of the standard wing were determined, after programming for the computer, by a matrix-iteration procedure, its steps being summed up shortly in the following.

____

* Since $p(z)$ depends on $m(z)$, the design has to be made by iteration; formulae (7) are quite suitable. These details of "static" design do not belong to the subject matter of the present paper.

Specific mass and second moment of area distribution of the standard wing are:

$$\left.\begin{array}{l} \bar{m} = [1 - (1 - \zeta)\bar{z}]^2 \\ \bar{J} = [1 - (1 - \zeta)\bar{z}]^4 \end{array}\right\} \tag{8}$$

The half-wing can be replaced by eight concentrated masses. According to Fig. 4a:

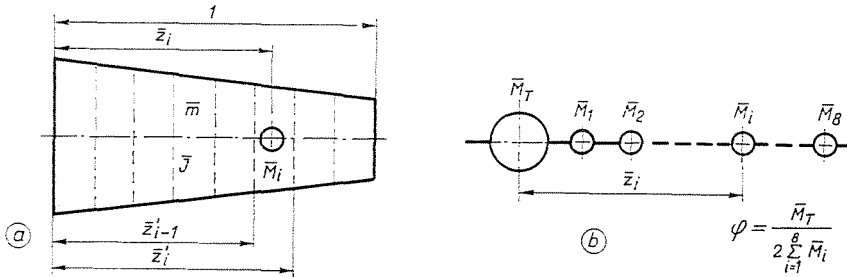$$M_i = \int_{\bar{z}_{i-1}}^{\bar{z}_i'} [1 - (1 - \zeta)\bar{z}]^2 \, d\bar{z} \qquad (i = 1, 2, \ldots, 8). \tag{9}$$

Fig. 4. Replacement of the wing by concentrated masses

The influence coefficients which can be inserted in the symmetrical square matrix $\bar{\mathbf{A}}$ will be calculated as follows:

$$\bar{a}_{ij} = \int_0^{\bar{z}_i} \frac{(\bar{z}_i - \bar{z})(\bar{z}_j - \bar{z})}{[1 - (1 - \zeta)\bar{z}]^4} \, d\bar{z} \quad (i \leq j; \ i, j = 1, 2, \ldots, 8). \tag{10}$$

The calculation by iteration of the first symmetrical, free eigenvibration can be started from the following matrix equation (Fig. 5):

$$\mathbf{y} - \mathbf{y}_T = \bar{\alpha}_1^2 \, \bar{\mathbf{A}} \, \bar{\mathbf{M}} \mathbf{y} = \bar{\alpha}_1^2 \, \bar{\mathbf{D}}^{(0)} \mathbf{y}, \tag{11}$$

where $\bar{\alpha}_1$ is the first dimensionless circular frequency, $\bar{\mathbf{M}}$ is the diagonal matrix of the masses replacing the half-wing (Fig. 4b), and $\bar{\mathbf{D}}^{(0)}$ is the so-called *dynamic*
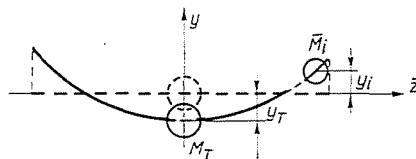

Fig. 5. Symbols for the calculation by iteration of the first eigenvibration

3*

matrix. y_T must be eliminated from Eq. (11), to render it suitable for iteration: this can be done according to the principle of mass-center. It can be shown that

$$y_T = -\,\bar{\alpha}_1^2 \frac{\displaystyle\sum_{i=1}^{8} \bar{A}_i\, y_i}{\bar{M}}\,, \tag{12}$$

where

$$\bar{A}_i = \sum_{i=1}^{8} \bar{a}_{ij}\, \bar{M}_i\, \bar{M}_j$$

and

$$\bar{M} = (1 + \varphi) \sum_{i=1}^{8} \bar{M}_i$$

(i.e., the mass of the half aircraft).

Thus the new matrix equation which can be directly iterated takes the following form:

$$\mathbf{y} = \bar{\alpha}_1^2\, \overline{\mathbf{D}}^{(1)}\, \mathbf{y}, \tag{13}$$

where

$$\overline{\mathbf{D}}^{(1)} = \begin{bmatrix} \bar{a}_{11}\bar{M}_1 - \dfrac{\bar{A}_1}{\bar{M}} & \bar{a}_{12}\bar{M}_2 - \dfrac{\bar{A}_2}{\bar{M}} & \ldots & \bar{a}_{18}\bar{M}_8 - \dfrac{\bar{A}_8}{\bar{M}} \\[2mm] \bar{a}_{21}\bar{M}_1 - \dfrac{\bar{A}_1}{\bar{M}} & \bar{a}_{22}\bar{M}_2 - \dfrac{\bar{A}_2}{\bar{M}} & \ldots & \bar{a}_{28}\bar{M}_8 - \dfrac{\bar{A}_8}{\bar{M}} \\[2mm] \vdots & \vdots & & \vdots \\[2mm] \bar{a}_{81}\bar{M}_1 - \dfrac{\bar{A}_1}{\bar{M}} & \bar{a}_{82}\bar{M}_2 - \dfrac{\bar{A}_2}{\bar{M}} & \ldots & \bar{a}_{88}\bar{M}_8 - \dfrac{\bar{A}_8}{\bar{M}} \end{bmatrix}. \tag{14}$$

The column-matrix obtained on the left-hand side will be normalized in every step of the iteration for the unit displacement of the mass $\bar{M}_8$. In the course of the iteration steps $\mathbf{y}$ will converge to the mode shape of the first eigenvibration normalized to the same place $(\eta^{(1)})$, while the normalizing factors will converge to $1/\bar{\alpha}_1^2$, i.e. to the inverse of the dimensionless firstcircular frequency-square.

For the calculation of the second eigenvibration the matrix sweeping out the first eigenvibration will take the following shape (as, besides ensuring the orthogonality of the two eigenvibrations, the principle of motion of mass-centre — i.e. the orthogonality to the rigid body-translation — must also be satisfied):

$$\overline{\mathbf{S}}^{(1)} = \begin{bmatrix} 0 & -\dfrac{\bar{M}_2(\eta_2^{(1)} - \eta_T^{(1)})}{\bar{M}_1(\eta_1^{(1)} - \eta_T^{(1)})} & -\dfrac{\bar{M}_3(\eta_3^{(1)} - \eta_T^{(1)})}{\bar{M}_1(\eta_1^{(1)} - \eta_T^{(1)})} & \ldots & -\dfrac{\bar{M}_8(\eta_8^{(1)} - \eta_T^{(1)})}{\bar{M}_1(\eta_1^{(1)} - \eta_T^{(1)})} \\[3mm] 0 & 1 & 0 & \ldots & 0 \\ \vdots & & & & \vdots \\ 0 & \cdot \quad \cdot \quad \cdot \quad \cdot & \cdot \quad \cdot \quad \cdot \quad \cdot & \cdot \quad \cdot \quad \cdot & 1 \end{bmatrix}. \tag{15}$$

Thus the matrix equation converging by iteration to the second free eigenvibration will be:

$$\mathbf{y} = \overline{\alpha}_2^2 \, \overline{\mathbf{D}}^{(1)} \, \overline{\mathbf{S}}^{(1)} \mathbf{y} = \overline{\alpha}_2^2 \, \overline{\mathbf{D}}^{(2)} \mathbf{y}, \tag{16}$$

Finally, the mode shapes $\eta^{(1)}$ and $\eta^{(2)}$ were transnormalized for the unit displacement of the root section in order to establish accordance with the foregoing:

$$\eta^{(1)\prime} = \frac{1}{\eta_T^{(1)}} \eta^{(1)} \quad \text{resp.} \quad \eta^{(2)\prime} = \frac{1}{\eta_T^{(2)}} \eta^{(2)}. \tag{17}$$

With an aircraft wing of standard wing character, featured by $s/2$, m_0, J_0 and E, the circular frequency can be obtained (for identical ζ and φ values) in the following way:

$$\alpha_i^2 = \frac{EJ_0}{m_0(s/2)^4} \overline{\alpha}_i^2 \quad (i = 1, 2), \tag{18}$$

while the normalized mode shapes remain unchanged.

The calculations were programmed for the Computer Type MINSK — 22 of the Research Institute of Automation of the Hungarian Academy of Sciences* for the taper ratio values: $\zeta = 0{,}25$; $0{,}35$ and $0{,}45$; and the mass ratio values: $\varphi = 1$; 2 and 3. A block scheme of the programme is shown in Fig. 6; the results are summarized in Tables I, II and III.

When examining an aircraft, in calculating the mass ratio φ, the fuel stored up in the wing must also be suitably considered beside the structural weight of the wing (its distribution is approximately proportional to the square of the cord ratio, as the wings nowadays are filled with fuel almost throughout their length); while the structural weight of the fuselage must be increased by the weight of the crew, payload (passengers, luggage etc.), the empennage surface and the weight of the rear-mounted engines, if any.

3. The dynamic load arising from landing

If an aircraft strikes the ground by its two main undercarriages at a certain vertical velocity, an impact force affects the undercarriages, and its changes with time can be estimated from the resilient characteristics of the undercarriage [5], while it can be considered as independent from the elastic properties of the aircraft itself [6]. These calculations are not dealt with here,
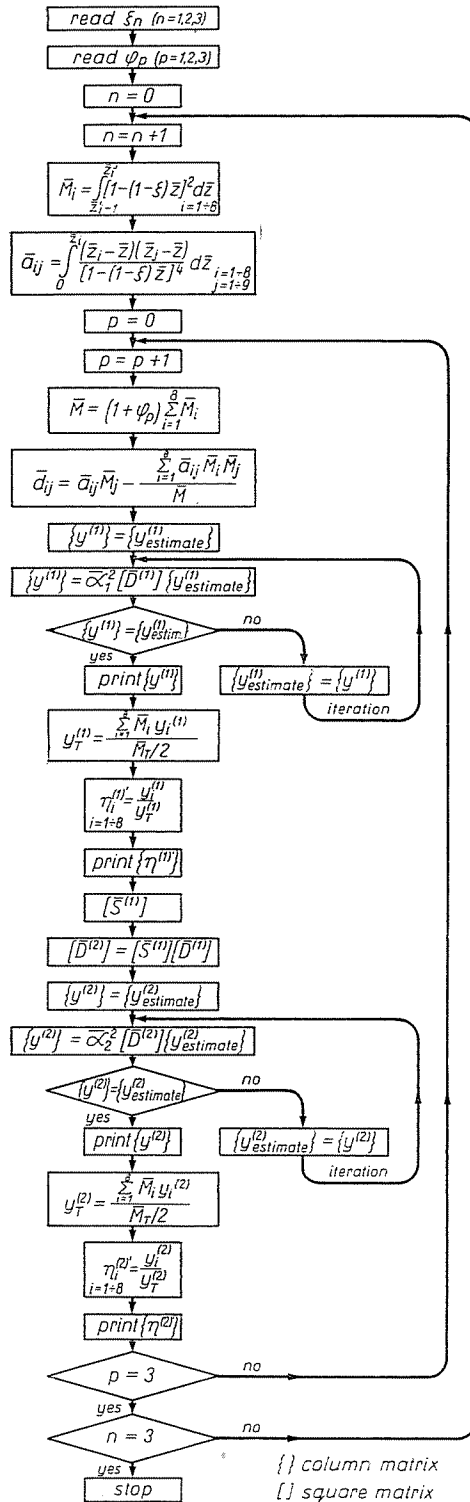
Fig. 6. Block diagram of the programme for calculating
normalized mode shapes and eigenfrequencies

Table I

Matrix of the influence coefficients. Normalized mode shapes and eigenfrequencies. Taper ratio: $\zeta = 0.25$

$$\bar{A} = \begin{bmatrix}
0.00009 & 0.00035 & 0.00061 & 0.00087 & 0.00113 & 0.00139 & 0.00165 & 0.00191 \\
0.00035 & 0.00256 & 0.00525 & 0.00795 & 0.01065 & 0.01334 & 0.01604 & 0.01873 \\
0.00061 & 0.00525 & 0.01329 & 0.02207 & 0.03086 & 0.03964 & 0.04843 & 0.05721 \\
0.00087 & 0.00795 & 0.02207 & 0.04155 & 0.06225 & 0.08295 & 0.10366 & 0.12436 \\
0.00113 & 0.01065 & 0.03086 & 0.06225 & 0.10262 & 0.14514 & 0.18767 & 0.23020 \\
0.00139 & 0.01334 & 0.03964 & 0.08295 & 0.14514 & 0.22362 & 0.30625 & 0.38888 \\
0.00165 & 0.01604 & 0.04843 & 0.10366 & 0.18767 & 0.30625 & 0.45771 & 0.61826 \\
0.00191 & 0.01873 & 0.05721 & 0.12436 & 0.23020 & 0.38888 & 0.61826 & 0.92516
\end{bmatrix}$$

z_i		0	1/16	3/16	5/16	7/16	9/16	11/16	13/16	15/16	$\bar{\alpha}$
$\bar{M}_i$			0.11365	0.09241	0.07336	0.05652	0.04187	0.02942	0.01917	0.01111	
$\varphi = 1.0$	$\eta_i^{(1)\prime}$	1.00000	0.96544	0.66239	−0.01549	−1.14833	−2.81304	−5.06489	−7.89983	−11.18112	6.36837
$\bar{M}_T/2 = 0.43750$	$\eta_i^{(2)\prime}$	1.00000	0.86913	−0.17537	−2.05061	−4.12233	−5.19856	−3.59055	2.34876	12.75080	19.7939
$\varphi = 2.0$	$\eta_i^{(1)\prime}$	1.00000	0.94643	0.48123	−0.54827	−2.25196	−4.73413	−8.06741	−12.23957	−17.05042	6.16276
$\bar{M}_T/2 = 0.87500$	$\eta_i^{(2)\prime}$	1.00000	0.80341	−0.89873	−3.85548	−7.01529	−8.46483	−5.56166	4.21740	21.00283	19.2931
$\varphi = 3.0$	$\eta_i^{(1)\prime}$	1.00000	0.92754	0.30089	−1.07937	−3.35358	−6.65418	−11.07190	−16.58677	−22.93485	6.06623
$\bar{M}_T/2 = 1.31250$	$\eta_i^{(2)\prime}$	1.00000	0.72582	−1.62004	−5.65415	−9.90052	−11.72580	−7.53196	6.08503	29.25851	19.0773

Table II

Matrix of the influence coefficients. Normalized mode shapes and eigenfrequencies. Taper ratio: $\zeta = 0.35$

$$
\overline{A} = \begin{bmatrix}
0.00008 & 0.00034 & 0.00060 & 0.00086 & 0.00112 & 0.00138 & 0.00163 & 0.00189 \\
0.00034 & 0.00250 & 0.00512 & 0.00774 & 0.01036 & 0.01297 & 0.01559 & 0.01821 \\
0.00060 & 0.00512 & 0.01277 & 0.02108 & 0.02939 & 0.03770 & 0.04601 & 0.05432 \\
0.00086 & 0.00774 & 0.02108 & 0.03901 & 0.05794 & 0.07687 & 0.09580 & 0.11473 \\
0.00112 & 0.01036 & 0.02939 & 0.05794 & 0.09352 & 0.13068 & 0.16784 & 0.20500 \\
0.00138 & 0.01297 & 0.03770 & 0.07687 & 0.13068 & 0.19583 & 0.26362 & 0.33141 \\
0.00163 & 0.01559 & 0.04601 & 0.09580 & 0.16784 & 0.26362 & 0.37890 & 0.49896 \\
0.00189 & 0.01821 & 0.05432 & 0.11473 & 0.20500 & 0.33141 & 0.49896 & 0.70312
\end{bmatrix}
$$

$\overline{z}_i$		0	1/16	3/16	5/16	7/16	9/16	11/16	13/16	15/16	$\overline{\alpha}$
$\overline{M}_i$			0.11512	0.09646	0.07944	0.06408	0.05037	0.03831	0.02790	0.01914	
$\varphi = 1.0$	$\eta_i^{(1)}$	1.00000	0.96732	0.68650	0.07582	−0.91158	−2.30839	−4.11763	−6.28970	−8.69717	5.82598
$\overline{M}_T/2 = 0.49083$	$\eta_i^{(2)}$	1.00000	0.86071	−0.23986	−2.11216	−4.03043	−4.85049	−3.24536	1.68551	9.45265	20.3341
$\varphi = 2.0$	$\eta_i^{(1)}$	1.00000	0.94946	0.51898	−0.40783	−1.89282	−3.97717	−6.65954	−9.86414	−13.40573	5.60868
$\overline{M}_T/2 = 0.98167$	$\eta_i^{(2)}$	1.00000	0.76902	−1.01819	−3.98840	−6.92693	−7.99576	−5.11651	3.07788	15.76048	19.7711
$\varphi = 3.0$	$\eta_i^{(1)}$	1.00000	0.93170	0.35227	−0.88983	−2.87210	−5.64480	−9.20270	−13.44397	−18.12510	5.50812
$\overline{M}_T/2 = 1.4725$	$\eta_i^{(2)}$	1.00000	0.76853	−1.80637	−5.90282	−9.89268	−11.22451	−7.04341	4.50304	22.24330	19.5574

Table III

Matrix of the influence coefficients. Normalized mode shapes and eigenfrequencies. Taper ratio: $\zeta = 0.45$

$$\overline{A} = \begin{bmatrix}
0.00008 & 0.00034 & 0.00060 & 0.00085 & 0.00111 & 0.00136 & 0.00162 & 0.00188 \\
0.00034 & 0.00245 & 0.00499 & 0.00757 & 0.01008 & 0.01263 & 0.01517 & 0.01771 \\
0.00060 & 0.00499 & 0.01228 & 0.02016 & 0.02804 & 0.03592 & 0.04380 & 0.05168 \\
0.00085 & 0.00754 & 0.02016 & 0.03676 & 0.05418 & 0.07159 & 0.08901 & 0.10643 \\
0.00111 & 0.01008 & 0.02804 & 0.05418 & 0.08590 & 0.11881 & 0.15172 & 0.18463 \\
0.00136 & 0.01263 & 0.03592 & 0.07159 & 0.11881 & 0.17418 & 0.23131 & 0.28844 \\
0.00162 & 0.01517 & 0.04380 & 0.08901 & 0.15172 & 0.23131 & 0.32324 & 0.41792 \\
0.00188 & 0.01771 & 0.05168 & 0.10643 & 0.18463 & 0.28844 & 0.41792 & 0.56704
\end{bmatrix}$$

$\bar{z}_i$		0	1/16	3/16	5/16	7/16	9/16	11/16	13/16	15/16	$\bar{\alpha}$
$\overline{M}_i$			0.11660	0.10060	0.08577	0.07213	0.05967	0.04839	0.03829	0.02938	
$\varphi = 1.0$	$\eta_i^{(1)}$	1.00000	0.96831	0.70148	0.13716	−0.74693	−1.95509	−3.46357	−5.21064	−7.09424	5.42424
$\overline{M}_T/2 = 0.55083$	$\eta_i^{(2)}$	1.00000	0.86361	−0.31408	−2.19667	−3.98718	−4.59497	−2.97482	1.32420	7.60813	20.9392
$\varphi = 2.0$	$\eta_i^{(1)}$	1.00000	0.95109	0.54263	−0.31313	−1.64253	−3.44623	−5.68531	−8.26769	−11.04544	5.19433
$\overline{M}_T/2 = 1.10167$	$\eta_i^{(2)}$	1.00000	0.77024	−1.15902	−4.17017	−6.92943	−7.67725	−4.77183	2.45490	12.85481	20.3373
$\varphi = 3.0$	$\eta_i^{(1)}$	1.00000	0.93397	0.38458	−0.76182	−2.53625	−4.93620	−7.90788	−11.32883	−15.00481	5.08918
$\overline{M}_T/2 = 1.65250$	$\eta_i^{(2)}$	1.00000	0.67970	−2.00247	−6.14381	−9.87628	−10.76847	−6.57670	3.58861	18.12410	20.0877

but for the sake of an approximate investigation the time history of the impact force is supposed to be sinusoidal:

$$P(t) = P_{max} \cdot F(t) = P_{max} \sin \frac{\pi}{T} t, \tag{19}$$

where T is the total time of the first in- and out closure of the shock strut.

It has also been shown theoretically and experimentally [7] that in the problem of landing the aerodynamic damping can be disregarded, since it affects but slightly the maximum value of the impact force with the first closure. The same study concludes that it is entirely satisfactory to consider
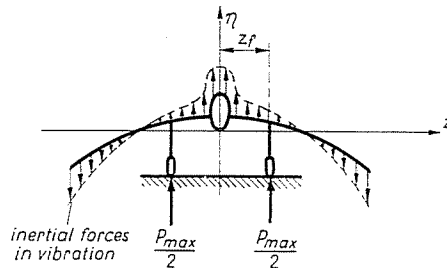

Fig. 7. Dynamic load on the wing in landing

the first three eigenvibrations for practical (design) purposes. (In this paper, for preliminary design, the first two eigenvibrations have been found sufficient.)

In the case of landing, the numerator of H_i [from (4)], obviously takes the form (Fig. 7):

$$\int\limits_{-s/2}^{+s/2} \frac{dP_{max}}{dz} \eta_i(z)\, dz = 2 \frac{P_{max}}{2} \eta_i(z_f), \tag{20}$$

i.e. it is nothing else but the (foreign) work done by the maximum impact force on the mode shape normalized for the unit displacement of the root section.

From this statement a significant conclusion can be drawn, hardly ever mentioned in the special literature. An overwhelming proportion of the dynamic load arises from the first eigenvibration. Now, if the undercarriage is attached to the wing at the nodal point of this mode shape (for $\eta_1(z_f) = 0$), the first eigenvibration does not add to the dynamic load, and thus it will be considerably lessened. (Roughly approximating the first mode shape by a quadratic parabola, and calculating the moment of inertia of the aircraft about its

longitudinal axis x from the mass elements of the wing only, it is easy to show that the radius of gyration i_x will be the proper location for attaching the undercarriage.)

In each cross-section of the wing the time-dependent shear force (positive upward) and flexural moment (positive when the bottom surface of the wing is in tension) can be written, according to Eqs. (4), (5) and (6), in the following form:

$$Q(z, t) = P_{\max} \left[- \frac{F(t)}{M} \int_z^{s/2} m'(z) \, dz + \bar{Q}_D(z, t) \right] \quad \text{if} \quad z > z_f \tag{21a}$$

and

$$Q(z, t) = P_{\max} \left[- \frac{F(t)}{M} \int_z^{s/2} m'(z) \, dz + \frac{F(t)}{2} + \bar{Q}_D(z, t) \right] \quad \text{if} \quad z < z_f, \tag{21b}$$

where

$$\bar{Q}_D(z, t) = \sum_{i=1}^{\infty} \frac{\eta_i(z_f) \int_z^{s/2} m'(z) \, \eta_i(z) \, dz}{2 \int_0^{s/2} m(z) \, \eta_i^2(z) \, dz} \left[\alpha_i \int_0^t F(\tau) \sin \alpha_i (t - \tau) \, d\tau - F(t) \right] \tag{21c}$$

or,

$$M(z, t) = P_{\max} \left[- \frac{F(t)}{M} \int_{s/2}^z \int_{s/2}^z m'(z) \, dz \, dz + \bar{M}_D(z, t) \right] \quad \text{if} \quad z > z_f \tag{22a}$$

and

$$M(z, t) = P_{\max} \left[- \frac{F(t)}{M} \int_{s/2}^z \int_{/2}^z m'(z) \, dz \, dz + \frac{F(t)}{2} (z_f - z) + \right.$$
$$\left. + \bar{M}_D(z, t) \right] \quad \text{if} \quad z < z_f, \tag{22b}$$

where

$$\bar{M}_D(z, t) = \sum_{i=1}^{\infty} \frac{\eta_i(z_f) \int_{s/2}^z \int_{s/2}^z m'(z) \, \eta_i(z) \, dz \, dz}{2 \int_0^{s/2} m(z) \, \eta_i^2(z) \, dz} \left[\alpha_i \int_0^t F(\tau) \sin \alpha_i (t - \tau) \, d\tau - F(t) \right]. \tag{22c}$$

$m'(z)$ is the specific mass of the wing.

Integration within the square brackets in (21c) and (22c) according to the time dependence of the impact force as shown in (20), yields:

$$\int\limits_0^t F(\tau) \sin \alpha_i (t - \tau)\, d\tau = \int\limits_0^t \sin \frac{\pi}{T}\, \tau \sin \alpha_i (t - \tau)\, d\tau =$$

$$= \frac{\dfrac{\pi}{T} \sin \alpha_i\, t - \alpha_i \sin \dfrac{\pi}{T}\, t}{\dfrac{\pi^2}{T^2} - \alpha_i^2}\,. \tag{23}$$

Formula (23) is valid only for the interval $t \leq T$, but in practice, the conditions usually work out so that the dynamic shear force and the flexural moment reach their maxima within this range.
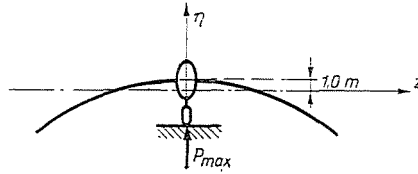

Fig. 8. Dynamic load on an aircraft with undercarriage attached to the fuselage

Let the above suggested method for preliminary wing design be employed for an aircraft, whose undercarriage is attached to the fuselage: $\eta_i(z_f) = \eta_i(0) = = 1.0$ (Fig. 8). Such are, for example, the sailplanes. Assuming the ultimate load on the wing to be due to "dynamic" landing the following procedure can be applied. First, the root section is designed for the ultimate static load (arising e.g. from gusts or pull out), according to the Design Requirements. Thus the J_0 and m_0 values are obtained. Knowing the natural frequencies and mode shapes of the standard wing, m_0 can be substituted into (21) and (22), and thus the flexural moment acting in the root section of the wing considered of standard characteristics is obtained (the same procedure goes for the shear force; it is not dealt with here). $P_{\max}$ written in the usual form $P_{\max} = nG = = ngM$ (n being the load factor in landing), we get:

$$M_0(t) = \mathrm{ng}\, \frac{s}{2} \left\{ - m_0\, \frac{s}{2} \sin \frac{\pi}{T}\, t \sum_{i=1}^8 \overline{M}_i \bar{z}_i + \right.$$

$$+ \frac{M}{2} \left[\frac{\displaystyle\sum_{i=1}^8 \overline{M}_i \eta_i^{(1)'} \bar{z}_i}{\dfrac{\overline{M}_T}{2} + \displaystyle\sum_{i=1}^8 \overline{M}_i \eta_i^{(1)'^2}} \left(\alpha_1\, \frac{\dfrac{\pi}{T} \sin \alpha_1 t - \alpha_1 \sin \dfrac{\pi}{T}\, t}{\dfrac{\pi^2}{T^2} - \alpha_1^2} - \sin \frac{\pi}{T}\, t \right) + \right.$$

$$+ \frac{\displaystyle\sum_{i=1}^8 \overline{M}_i \eta_i^{(2)'} \bar{z}_i}{\dfrac{\overline{M}_T}{2} + \displaystyle\sum_{i=1}^8 \overline{M}_i \eta_i^{(2)'^2}} \left.\left.\left(\alpha_2\, \frac{\dfrac{\pi}{T} \sin \alpha_2 t - \alpha_2 \sin \dfrac{\pi}{T}\, t}{\dfrac{\pi^2}{T^2} - \alpha_2^2} - \sin \frac{\pi}{T}\, t \right) \right]\right\}, \tag{24}$$

where α_1 and α_2 can be calculated according to formula (19).

Let us denote:

$$A = \sum_{i=1}^{8} \overline{M}_i \bar{z}_i, \; B_1 = -\; \frac{\sum\limits_{i=1}^{8} \overline{M}_i \eta_i^{(1)'} \bar{z}_i}{\dfrac{\overline{M}_T}{2} + \sum\limits_{i=1}^{8} \overline{M}_i \eta_i^{(1)'2}}\; , \; B_2 = -\; \frac{\sum\limits_{i=1}^{8} \overline{M}_i \eta_i^{(2)'} \bar{z}_i}{\dfrac{\overline{M}_T}{2} + \sum\limits_{i=1}^{8} \overline{M}_i \eta_i^{(2)'2}}\; ,$$

$$F_1(t) = \frac{\dfrac{\pi}{T} \sin \alpha_1 t - \alpha_1 \sin \dfrac{\pi}{T} t}{\dfrac{\pi^2}{T^2} - \alpha_1^2} - \sin \dfrac{\pi}{T} t,$$

$$F_2(t) = \frac{\dfrac{\pi}{T} \sin \alpha_2 t - \alpha_2 \sin \dfrac{\pi}{T} t}{\dfrac{\pi^2}{T^2} - \alpha_2^2} - \sin \dfrac{\pi}{T} t.$$

Thus:

$$M_0(t) = -\; \text{ng} \frac{s}{2} \left\{ A \frac{s}{2} m_0 \sin \frac{\pi}{T} t + \frac{M}{2} \left[B_1 F_1(t) + B_2 F_2(t) \right] \right\} \dots (25)$$

The values of A, B_1 and B_2 from the numerical data in Tables I through III. are summarized in Table IV.

Table IV

ζ	φ	A	B_1	B_2
	1.0		0.09668	0.03286
0.25	2.0	0.14185	0.06783	0.02130
	3.0		0.05202	0.01571
	1.0		0.11897	0.03336
0.35	2.0	0.17343	0.07989	0.02137
	3.0		0.06112	0.01554
	1.0		0.13191	0.03297
0.45	2.0	0.21000	0.09172	0.02084
	3.0		0.07003	0.01517

The simplest way to obtain the maximum of $M_0(t)$ in time is to plot the expression (25) (Fig. 9). Therefrom, the initial data of the next step in the iteration can easily be obtained:

$$J_1 = J_0\,\beta_M = J_0\,\frac{M_0\,(t)_{max}}{M_{0st}}$$

where M_{0st} is the root moment from the ultimate static load.

β_M rapidly converges to its final value: β_M^*. If the distribution of the flexural moment derived from the static load is multiplied by β_M^* (that is, shear force distribution multiplied by β_Q^*), the final structural design of the wing can be accomplished.

It must be noted that the dynamic load is significant not only in the root section but also in the sections along the wingtip, while it is smaller in
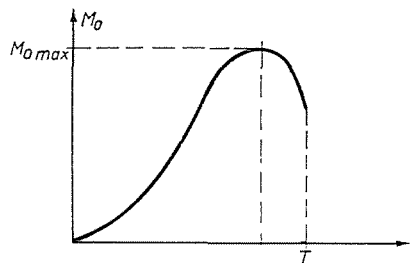

Fig. 9. Time history of the "dynamic" flexural moment of the root section

the sections about the nodal point of the first mode shape. The factor β_M^* will, however, have a favourable effect on the stress distribution at the wingtip as well, the latter being generally overdimensioned.

The wing thus shaped must finally undergo a detailed dynamic examination according to the above considerations, but in this case with due regard to the actual $m(z)$ and $J(z)$ distributions; but there is good reason to hope that, as a result of the approximation described above, there will be no need for a major structural re-shaping.

Summary

Earlier, the airplane wings had been designed as rigid constructions subject to "static" loads: acting forces and balancing inertia forces. Upon an abrupt load increase (gusts, landing impacts), however, the wings begin to vibrate, and arising inertia forces produce a dynamic overload. To reduce the involved tedious computation work in estimating the dynamic load in landing, notion of the "standard" wing has been introduced, for which the mass distribution and the second moment of area are proportional to the square and to the fourth power of the chord ratio, respectively. For the preliminary design of the wing a quickly converging method has been presented, based on the use of predetermined vibration data (eigenfrequencies, flexural mode shapes) of the standard wing.

References

1. Rácz, E.: (Editor) Repülőgéptervezés I. rész. Tankönyvkiadó, Budapest 1955.
2. Williams, D.: An introduction to the theory of aircraft structures. Edward Arnold Ltd., London 1960.
3. Bisplinghoff, R. L.—Ashley, H.—Halfman, R. L.: Aeroelasticity. Addison-Wesley, Cambridge, Mass., 1955
4. Ramberg, W.: Transient Vibration in an airplane wing obtained by several methods. Research Paper RP 1984 V. 42. N. 5. 1949. National Bureau of Standards.
5. Rácz, E.: (Editor) Repülőgépek szerkezete és rugalmassága. Tankönyvkiadó, Budapest, 1962.
6. Mc. Pherson, A. E.— Evans, J. Jr.— Levy, S.: Influence of wing flexibility on force-time relation in shock strut following vertical landing impact. NACA T. N. 1955 (1954).
7. Pian, T. H. H.— Flamenhoft, H. I.: J. Ae. Sc. **17**, 765 (1950).

Prof. Dr. Elemér Rácz, Budapest XI., Bertalan Lajos u. 4—6. Hungary